Heliyon 10 (2024) e23222

Contents lists available at ScienceDirect

Heliyon

journal homepage: www.cell.com/heliyon

A novel inhibitor of SARS-CoV infection: Lactulose octasulfate interferes with ACE2-Spike protein binding

Rami Adel Pashameah [a,**], Raya Soltane [b], Ahmed M. Sayed [c,d,*]

[a] Department of Chemistry, Faculty of Applied Science, Umm Al-Qura University, Makkah 21955, Saudi Arabia
[b] Department of Biology, Adham University College, Umm Al-Qura University, Makkah 21955, Saudi Arabia
[c] Department of Pharmacognosy, Faculty of Pharmacy, Nahda University, 62513 Beni-Suef, Egypt
[d] Department of Pharmacognosy, collage of Pharmacy, Almaaqal University, 61014 Basra, Iraq

ARTICLE INFO

Keywords:
COVID-19
Spike protein
MD simulation
Sulfated carbohydrates
*Ga*MD
Bio-layer interferometry

ABSTRACT

The ongoing challenge of managing coronaviruses, particularly SARS-CoV-2, necessitates the development of effective antiviral agents. This study introduces Lactulose octasulfate (LOS), a sulfated disaccharide, demonstrating significant antiviral activity against key coronaviruses including SARS-CoV-2, SARS-CoV, and MERS-CoV. We hypothesize LOS operates extracellularly, targeting the ACE2-S-protein axis, due to its low cellular permeability. Our investigation combines biolayer interferometry (BLI), isothermal titration calorimetry (ITC)-based experiments with in silico studies, revealing LOS's ability to reduce SARS-CoV-2's RBD's affinity for ACE2 in a dose-dependent manner, and bind tightly to ACE2 without inhibiting its enzymatic activity. Gaussian accelerated molecular dynamics simulations (*Ga*MD) further supported these findings, illustrating LOS's potential as a broad-spectrum antiviral agent against current and future coronavirus strains, meriting in vivo and clinical exploration.

1. Introduction

The battle against the highly infectious COVID-19 has reached a pivotal point since its initial detection in December 2019. As of June 2023, the pandemic has led to over 690 million cases and an estimated 6.8 million fatalities [1,2]. The World Health Organization has recently declared that COVID-19 is no longer considered an emergency situation. However, it remains crucial to maintain vigilance in curbing the spread of new, highly transmissible variants of the SARS-CoV-2 virus. In addition, it's imperative for pharmaceutical companies and research institutions globally to focus on the development of versatile antiviral drugs to better equip us for future pandemics [3].

Structurally, SARS-CoV-2 virus is a sphere with spike-like projections. The spike glycoprotein (S-protein) of corona viruses controls their entrance into human host cells [4]. Extensive alveolar damage reported in corona viruses (e.g., SARS-CoV, SARS-CoV-2, and MERS-CoV) infections may be explained by the fact that these viruses target alveolar cells in the lungs by binding with their angiotensin converting enzyme type 2 (ACE2) [5].

Remdesivir, an antiviral medication, along with dexamethasone, a wide-ranging anti-inflammatory drug, have demonstrated effectiveness in lowering hospital admissions and duration of hospital stays for patients with respiratory failure needing support due to

* Corresponding author. Department of Pharmacognosy, Faculty of Pharmacy, Nahda University, 62513 Beni-Suef, Egypt.
** Corresponding author. Department of Chemistry, Faculty of Applied Science, Umm Al-Qura University, Makkah 21955, Saudi Arabia.
E-mail addresses: rapasha@uqu.edu.sa (R.A. Pashameah), rasoltan@uqu.edu.sa (R. Soltane), Ahmed.mohamed.sayed@nub.edu.eg (A.M. Sayed).

https://doi.org/10.1016/j.heliyon.2023.e23222
Received 14 October 2023; Received in revised form 28 November 2023; Accepted 29 November 2023
Available online 3 December 2023

cytokine storms [6–9]. Additionally, nirmatrelvir, an orally administered 3C-like protease inhibitor commonly known as Paxlovid, when used in combination with ritonavir, has also proven to be an effective oral treatment for COVID-19 [10].

Patients with COVID-19 may benefit from blocking the action of ACE2, a dipeptidylcarboxypeptidase that is an integral membrane protein [11]. Recent reports have shown that the ACE2 receptor is essential for the spread of coronaviruses [12]. The spike protein of SARS-CoV binds to the host ACE2 receptor, allowing the virus to reach its intended cells. The genome of SARS-CoV-2 is 82 % similar to that of SARS-CoV. The similarity between their receptor binding domains (RBD) indicates that they share a common entry mechanism via the ACE2 receptor [13].

The corona viruses spike protein has been shown to directly bind to ACE2 with high affinity by several cryo-electron microscopy experiments [14]. Targeting ACE2 may be an efficient technique for the development of antiviral medications, as soluble human ACE2 was recently reported to inhibit early stages of SARSCoV-2 infection in engineered human tissues [15].

However, the effectiveness of ACE2 inhibitors/angiotensin receptor blockers in the treatment of patients with COVID-19 has not been established by conclusive data from large-scale clinical research [16].

Hence, finding a suitable ACE2 blocker is considered a very interesting starting point for the development of broad-spectrum anti corona virus agents that can help in the current situation and will be of great importance in the next coronavirus pandemic.

Accordingly, we initiated a screening campaign to develop coast-effective S-protein and/or ACE2 blockers based on the accumulating reports of the efficacy of sulfated polysaccharides and sulfated oligosaccharides in this regard [17–19].

Both in vitro and in vivo studies have shown that sulfated polysaccharides and their derivatives effectively suppress SARS CoV-2, with only a small percentage of resistant virus strains emerging over time [20,21]. These drugs primarily impede viral entry by binding to the viral receptor-binding domain (RBD) or host ACE2, or both [22–26]. It has been observed that heparin, a naturally occurring sulfated polysaccharide anticoagulant, can efficiently inhibit SARS CoV-2 through the same mechanism [20].

Recent molecular dynamics simulation studies have identified a distinct binding site at the juncture of the SARS-CoV-2 Receptor Binding Domain (RBD) and the human ACE2 receptor (referred to as Site A). Introducing a suitable ligand, such as Aloin A, into this site resulted in the destabilization and subsequent complete dissociation of the RBD-ACE2 complex [27].

The primary objective of this study is to investigate the antiviral efficacy of Lactulose octasulfate (LOS) against key coronaviruses, including SARS-CoV-2, with a focus on its mechanism of action and potential as a broad-spectrum antiviral agent. This involves evaluating LOS's ability to interfere with the ACE2-S-protein interaction, a critical step in coronavirus infection, using a combination of biolayer interferometry, isothermal titration calorimetry, and advanced molecular dynamics simulations. The schematic overview provided encapsulates the key findings of this study.

2. Methods

2.1. Chemical substances

In this research, all the sulfated oligosaccharides (SOS), were semi-synthesized by applying a sulfation process to their unsulfated precursors, acquired from Sigma Aldrich™, using a previously documented method [28]. We utilized ^{1}H NMR, ^{13}C NMR, and elemental analysis techniques to characterize the synthesized derivatives. Notably, SOS and other compounds maintained their solubility even when diluted in cell culture medium.

2.2. In vitro-based assays

2.2.1. Antiviral assay

2.2.1.1. Virus and cells. The Vero-E6 cells were meticulously maintained in a controlled environment at 37 °Cand an atmosphere containing 5 % carbon dioxide (CO_2), utilizing Invitrogen technology. For their sustenance and growth, these cells were cultured in Dulbecco's Modified Eagle's Medium (DMEM), which was further enriched with a combination of 2 % penicillin/streptomycin and 10 % bovine serum, ensuring optimal conditions for cellular health and viability. Following a 24-h incubation in tissue culture flasks using an infection medium containing 4 % BS and 1 % trypsin treated with L-1-tosylamido2-phenylethyl chloromethyl ketone (TPCK), the cells were exposed to various coronavirus strains. These included SARS CoV-2, SARS-CoV, or MERS-CoV isolates, specifically hCoV-19/Egypt/NRC-3/2020 (with the GSAID Accession Number EPI_ISL_430820) and NRCE-HKU270 (Accession Number: KJ477103.2), to produce virus stocks. The infected media were changed out for new medium containing the viral inoculum after 2 h, and the incubation period was extended for another three days. To get rid of any remaining debris, we centrifuged the cells for 5 min at 2500 rpm before collecting the supernatant. The supernatant, once aliquoted and transferred into a new 50 mL Falcon tube, was subjected to titration through a plaque infectivity assay.

2.2.1.2. MTT cytotoxicity assay. To find the IC_{50} for preliminary antiviral screening, DMEM was used to dilute stock solutions of the test compounds in 10 % DMSO with double distilled water. Vero-E6 cells were employed in the 3-(4,5-dimethylthiazol-2-yl)-2,5-diphenyltetrazolium bromide (MTT) assay [29] to ascertain the cytotoxic effect of the test substances. The cells were cultured for 24 h at 37 °C with 5 % CO_2 after being seeded at 3105 cells/mL into 100 μL/well in 96-well plates. The cells were tested at three different concentrations for 24 h. After 24 h, the supernatant was discarded and the cell monolayers were washed three times with sterile PBS. 20 μL of the 5 mg/mL stock MTT solution was added to each well, and the plates were incubated at 37 °C for 4 h. The produced

formazan crystals were dissolved in 200 μL of acidified isopropanol (0.04 μM HCl in 100 % isopropanol = 0.073 mL HCL in 50 mL isopropanol). The absorbance of the formazan solutions was measured after optimizing the wavelength of the microplate reader to 540 nm. The relative cytotoxicity of treated cells compared to untreated cells was determined using the following formula:

$$\%\ \text{Cytotoxicity} = \frac{(\text{absorbance of cells without treatment} - \text{absorbance of cells with treatment})\ x\ 100}{\text{absorbance of cells without treatment}}$$

We plotted the cytotoxicity percentage versus the sample concentrations to derive the IC_{50} values. The positive control drug was doxorubicin (IC_{50} = 22.43 0.24 μM).

2.2.1.3. Assessment of viral replication. 2.4 x 10^4 Vero-E6 cells were seeded into each well of a 96-well plate, and the plates were incubated at 37 °C with 5 % CO_2 for 24 h. After one wash with PBS, we let viruses adhere to cell monolayers at room temperature for an hour. Then, 50 μL of DMEM containing the test compounds at varying doses was applied to the cell monolayers. After being fixed in 100 mL of 4 % paraformaldehyde for 20 min, cells were stained for 15 min with 0.1 % crystal violet. By utilizing an Anthos Zenyth 200 rt plate reader (Anthos Labtec Instruments, Heerhugowaard, The Netherlands), we were able to determine the produced color at 570 nm. Each well had 100 μL of crystal violet dissolved in methanol put to it. The "IC_{50}" of the drug is the concentration at which the virus-induced cytopathic effect (CPE) is reduced by 50 %. Remdesivir was used as a positive control.

2.2.2. Bio-layer interferometry (BLI) assay

The biosensors and ForteBio Octet RED96 device were used to determine BLI. The retrieved data was analyzed using ForteBio Data Analysis 9.0. Kinetics experiments were performed using a sample plate shake speed of 1000 rpm and a temperature of 25 °C degrees Celsius.

Acrobiosystems provided the human ACE2 in its purified form and the SARS-CoV-2 RBD with a His-tag. For the experiments, 200 nM of the His-tagged RBD protein was utilized to load onto Ni-NTA sensors. This study aimed to explore the interaction between RBD and ACE2 by introducing varying concentrations of ACE2 to the sensors, both in the absence and presence of different levels of the tested sulfated oligosaccharide, such as LOS. During the dissociation phase, the sensors, once bound, were re-immersed in the wells to monitor baseline time progression. The resulting binding curves were then analyzed to determine kinetic and thermodynamic parameters, including the rate constants of association (ka), dissociation (kd), and the equilibrium dissociation constant (KD).

2.2.3. Isothermal titration calorimetry

We used isothermal titration calorimetry (ITC) to determine how strongly LOS binds to ACE2 and RBD. A MicroCal Automated-iTC200 calorimeter (Malvern, UK) was used to carry out the calorimetric titrations. Each protein (10 μM) was titrated by adding 100 μM of LOS. Both phosphate (i) 50 μM, pH 7, with 1 % DMSO, and Tris (ii) 50 μM, pH 7, with 1 % DMSO, were used as buffer solutions for the experiments. The treatments included 27 injections of 2 μL each, with 150 s between injections and a stirring speed of 750 rpm. In this case, 10 μcal/s of reference power was used. Non-linear least-squares regression analyses were performed on the collected data in Origin 7.0 (OriginLab, Northampton, MA, USA) to calculate the binding enthalpy (ΔH), the binding stoichiometry (n), the association constant (*K*a), and Gibbs's free energy, or the binding free energy (Δ*G*). Using the measured thermodynamic properties, we determined the dissociation constant, K_d, and the binding entropy, -TS. A linear regression of the detected enthalpy as a function of the ionisation enthalpy for the buffer solution H_{buf} (H═H0 + nH H_{buf}) was used to determine the buffer-independent enthalpic, H0, and entropic contribution, -TS0, and the number of exchanged protons upon formation of the ligand-enzyme complex (nH).

2.2.4. Assay for ACE2 enzymatic activity

Experiments to test enzyme inhibition were conducted using a human ACE2 assay kit (Catalogue #: ab273373, Abcam, USA), adhering strictly to the guidelines provided by the manufacturer. In these experiments, MLN-4760 was used as a positive control. The assay involves measuring the fluorescence emitted by the enzyme upon substrate cleavage, which can be quantified using a microplate reader at wavelengths of 460 nm for emission and 360 nm for excitation. After adding 10 μL of test compounds of varied concentrations to a 96-well plate, the enzyme was diluted to a final concentration of 15 μg/mL in 30 μL. The results of the room-temperature incubations were examined after 30 min. A total of 50 μL of substrate and 10 μL of reaction buffer were mixed and applied to each well to achieve a final concentration of 40 μM. The resulting mixture was heated in a n incubator at 20 °C for 4 h. A microplate-reading fluorimeter was used to measure the amount of fluorescence produced.

2.3. Cellular uptake of LOS

We used the same approach as in Ref. [22] to estimate the amount of LOS taken in by cells. For 4 h, Vero-E6 cells were cultured in full media containing 5 μM desalted LOS. The concentrations of LOS within and outside the cells were then measured. To get rid of any remaining media, we gave the cells two PBS washes. Then, (i) 200 μl of lysis buffer and 200 μl of PBS were used to lyse the cells and wash the wells, and (ii) 500 μL of 1 M NaCl was added to the cells after they had been spun down at 1500 rpm for 5 min to extract the LOS. As a control, we used 500 μL of 10 μM emodin in 80 % methanol (a compound that can be quickly accumulated inside the cell) [23].

After 15 min in the refrigerator, the samples were broken up and centrifuged at 10,000 revolutions per minute for 10 min to remove excess liquid. The proteins that precipitated out were discarded while the supernatants were saved for HPLC analysis. HPLC equipment (Agilent Corporation, Germany) equipped with a Photodiode Array Detector was used for the chromatographic separation. We used an

RP C18 column (250 mm 4.6 mm 4.5 μm, Waters Corporation, Milan, Italy) to separate the compounds. We used a linear methanolic gradient with a flow rate of 1 mL/min and a concentration range of 20 % v/v to 80 % v/v over the course of 15 min (A: water for HPLC with HCl to achieve pH of 3.5, and B: 1 M NaCl solution with HCL to reach a pH of 3.5). Compounds having peaks between 210 and 400 nm were identified by comparing retention time and spectra to those of LOS and emodin standards [22].

To determine the quantities of individual compounds in the medium and the cell lysate, standard stock solutions were produced in 1 M NaCl (80 % methanol for emodin), filtered, and diluted to the desired concentrations (1.0, 5.0, 10.0, and 20.0 μM). By comparing the experimental data to reference calibration curves, the compound concentrations in the extracellular and intracellular fluids were determined. Results from a protein assay were obtained and expressed as nmol of LOS or emodin per mg of protein, as previously published [22,23].

2.4. In silico and molecular dynamics investigations

The details of docking, MD simulation, binding free energy calculations, and GaMD experiments are described in the supplementary file, Pages: 9 and 10.

3. Results

3.1. In vitro results

To expand upon our previous SARS-CoV-2-related research, we have initiated extensive in vitro and in silico investigations to identify potential candidates among sulfated mono- and disaccharides that are effective against SARS-CoV-2. The RBD-ACE2 complex of SARS CoV-2 is a promising target, particularly for low-permeability compounds such as aloin A and sulfated polysaccharides [27, 24]. The discovery of a conserved binding site (Site A) between the two proteins is also depicted in Fig. 4A. Extensive MD simulation studies indicated that ligand interaction with this site can induce dissociation of the complex [27].

The primary objective of the present study is to identify potential sulfated oligosaccharides capable of binding with human ACE2 at the binding location where SARS CoV spike protein attaches.

Due to the rapid and continuous mutation of RNA viruses, including SARS CoV, targeting ACE2 without interfering with its biological function is more advantageous than targeting the viral spike protein or any other targets.

ACE2 is the primary entry point for SARS CoV [25] into the host cell; consequently, blocking this essential host-specific receptor with antibodies or other binders has been shown to provide substantial protection against viral infection and spread [26,30,31].

Therefore, this ACE2-blocking strategy by sulfated oligosaccharides will provide cost-effective, broad-spectrum preventive agents to protect against or even treat SARS CoV-related infections, especially during the next pandemic.

Several products containing sulfated polysaccharides have been utilized as broad-spectrum antiviral agents [32,33].

Heparan sulfate and its oligosaccharide derivatives, such as pixatimod, inhibit several SARS CoV-2 variants by preventing their cellular entry via the S-protein-ACE2 axis [34]. In addition, sulfated abalone polysaccharide destabilizes the S-protein-ACE2 complex,

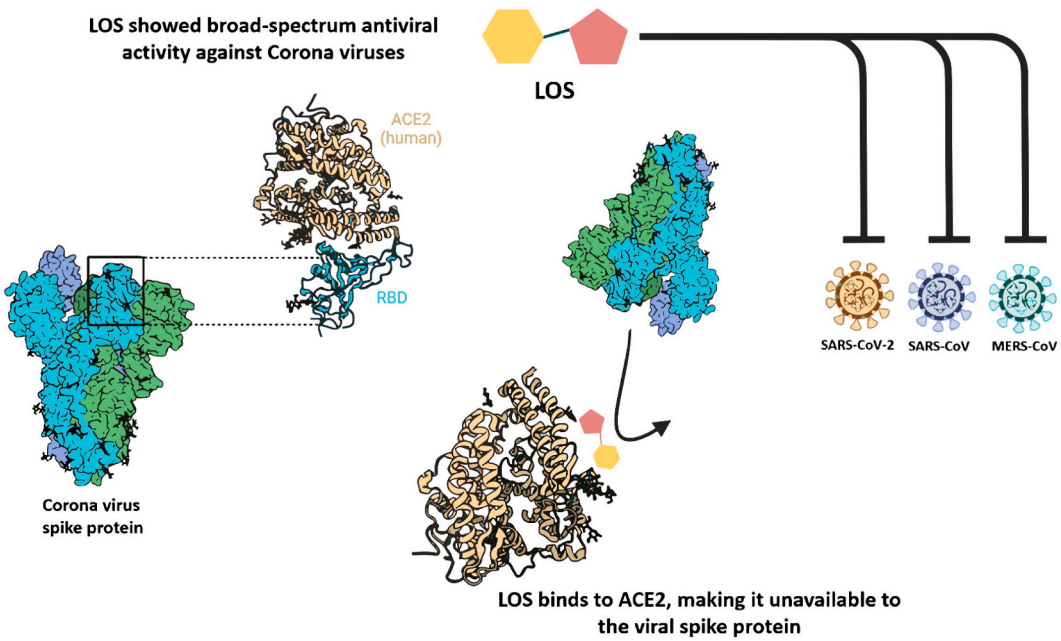

Fig. 1. Summary diagram of the findings of the current investigation.

resulting in a weak association and, consequently, significant antiviral activity against multiple variants of SARS CoV-2 [35].

3.1.1. LOS have a broad-spectrum antiviral activity against coronaviruses

In contrast to Sulfated polysaccharides, Sulfated disaccharides, particularly sulfated oligosaccharides, have much better stability and less side effects (i.e., anticoagulant effect). In addition, it much easier in their preparation (i.e., cost-effective).

Therefore, we prepared a small library of Sulfated disaccharides by sulfonating their corresponding parent disaccharides [36]. Then, we tested them against the coronavirus (see Fig. 1).

From this small library, lactulose octasulfate (LOS) showed interesting antiviral activity against SARS CoV-2 strain with an IC_{50} value of 4.62 ± 0.32 μM. Additionally, it was also active against SARS CoV and MERS CoV with IC_{50} values of 5.35 ± 0.21 and 3.93 ± 0.27 μM (Fig. 2A). All of these antiviral assays measured how LOS protected Vero E6 cells against the cytopathic effect of each coronavirus (i.e., plaque reduction assay).

Regarding the cytotoxicity of LOS, it showed minimal toxicity towards Vero E6 cells with CC_{50} of 139.46 ± 2.56 μM.

3.1.2. The transport of LOS across the cell membrane is quite poor

Cellular permeability of LOS was evaluated to determine its subcellular localization. Vero-E6 cells were incubated with 5 μM LOS for 4 h, after which the extracellular and intracellular concentrations of LOS were measured. The intracellular concentration of LOS was determined to be undetectable, while the extracellular concentration was 4.31 ± 0.18 μM.

These results provide further evidence that LOS antiviral action against SARS CoV-2 occurs via an extracellular mechanism, (i.e., via the S-protein/ACE2 axis).

LOS's S-protein/ACE2 interaction is possibly the primary mechanism for its antiviral activity because its high hydrophilicity and negatively charged nature prevent its transport across the cellular membrane.

3.1.3. The binding of S-protein to ACE2 is directly inhibited by LOS

The interaction strength, quantified as the equilibrium dissociation constant (KD), between the S-protein Receptor Binding Domain (RBD) and ACE2 was evaluated using a biolayer interferometry-based assay. This assessment was conducted both in the absence and presence of LOS to determine whether LOS influences this specific interaction. Fig. 2B and C demonstrate that the affinity for ACE2 considerably reduced upon the addition of LOS at varying doses. There was no detectable binding signal at 800 nM. These results provided substantial support for the suggested anti-SARS CoV-2 mechanism of LOS.

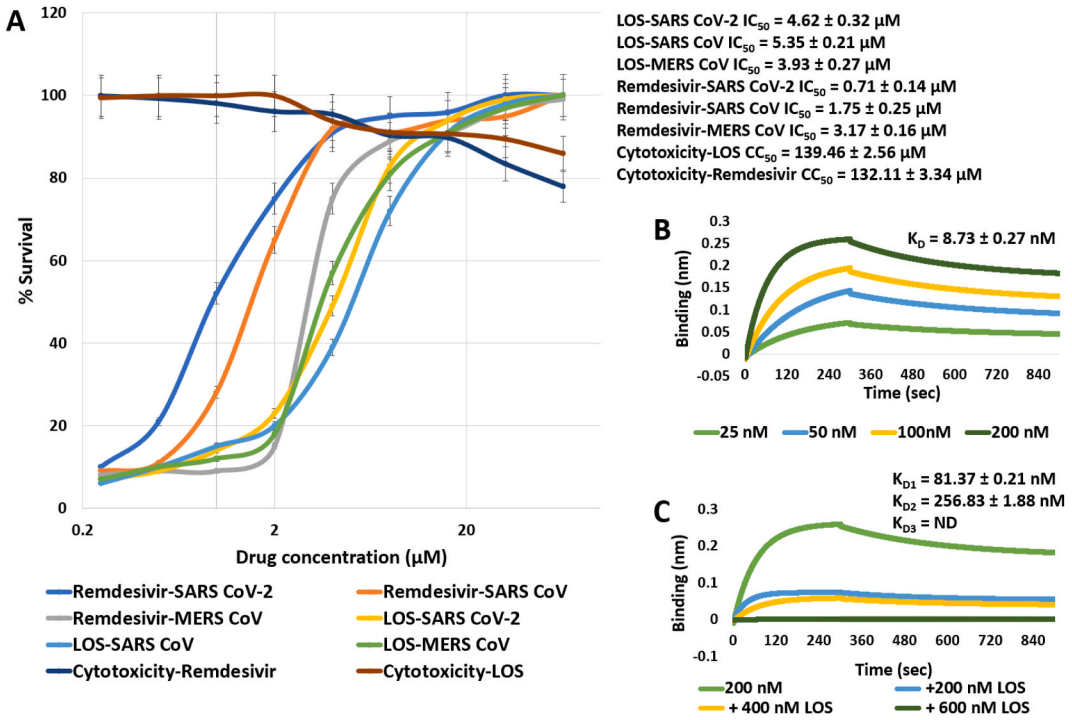

Fig. 2. A: shows the IC_{50} and CC_{50} values for LOS's inhibitory activity and cellular cytotoxicity against SARS CoV-2, SARS CoV, and MERS CoV replications, respectively. As a positive control, we used remdesivir. Bio-layer interferometry (BLI) was used to assess the dissociation constants (K_D) of RBD-ACE2 in the absence and presence of LOS at various concentrations (B and C, respectively). The K_D values of RBD-ACE2 at LOS concentrations of 200 nM, 400 nM, and 600 nM are denoted as K_{D1}, K_{D2}, and K_{D3}, respectively. Not Known; ND. Octet Data Analysis was used to calculate KD values.

3.1.4. LOS binds with ACE2 but not with RBD

To check if LOS binds with SARS CoV-2's RBD or with ACE2 or both, two independent isothermal titration calorimetry (ITC) experiments were carried out. The resulting thermodynamic data (Fig. 3) from both experiments indicated clearly that LOS can bind with ACE2 only.

Hydrogen bonding is likely the key interaction involved in the binding of LOS and ACE2, as shown by the thermodynamic data, which indicate favorable enthalpy ($\Delta H = -13.67$ kcal/mol). The compensatory unfavorable entropy ($-T\Delta S$) on the other hand was 2.13 kcal/mol. Hence the overall binding affinity (ΔG) of LOS with ACE2 was −11.54 kcal/mol, and the dissociation constant (KD) was 5.28 nM.

The K_D of SARS CoV-2 RBD-ACE2 binding was determined to be 8.73 nM (Fig. 2B) and this value was comparable to the previously reported one by Wang et al., 2020 [37] ($K_D = 8.02$ nM), indicating that LOS has a higher affinity for ACE2 than the RBD.

3.1.5. LOS does not inhibit ACE2 activity

The in vitro LOS inhibitory action against human ACE2 was investigated to see if LOS binding impacts the catalytic activity of ACE2. The enzyme's activity was found to be unaffected by LOS up to 100 μM. As a result, it is possible to conclude that LOS interacts with ACE2 via an allosteric binding site (rather than the active site), and that this binding has no influence on the enzyme's physiological activity.

3.2. Modeling study

According to the previous in vitro study, LOS can bind with human ACE2 in a way that prevents SARS CoV-2 RBD from establishing a tight interaction with the enzyme, which explains LOS's broad-spectrum antiviral activity against the common coronavirus members, making this sulfated disaccharide a very interesting viral independent anti-corona virus candidate.

To get insight into the possible mode of interaction of LOS with ACE2, we carried out a number of modeling-based and biophysics simulation-based experiments. In addition, we simulated the binding event of LOS with ACE2 using Gaussian accelerated molecular dynamics (*Ga*MD).

3.2.1. LOS does not destabilize RBD-ACE2 complex

In our previous study, we reported that binding of aloin A (i.e., a plant natural product) into a binding site (Site A) located at the

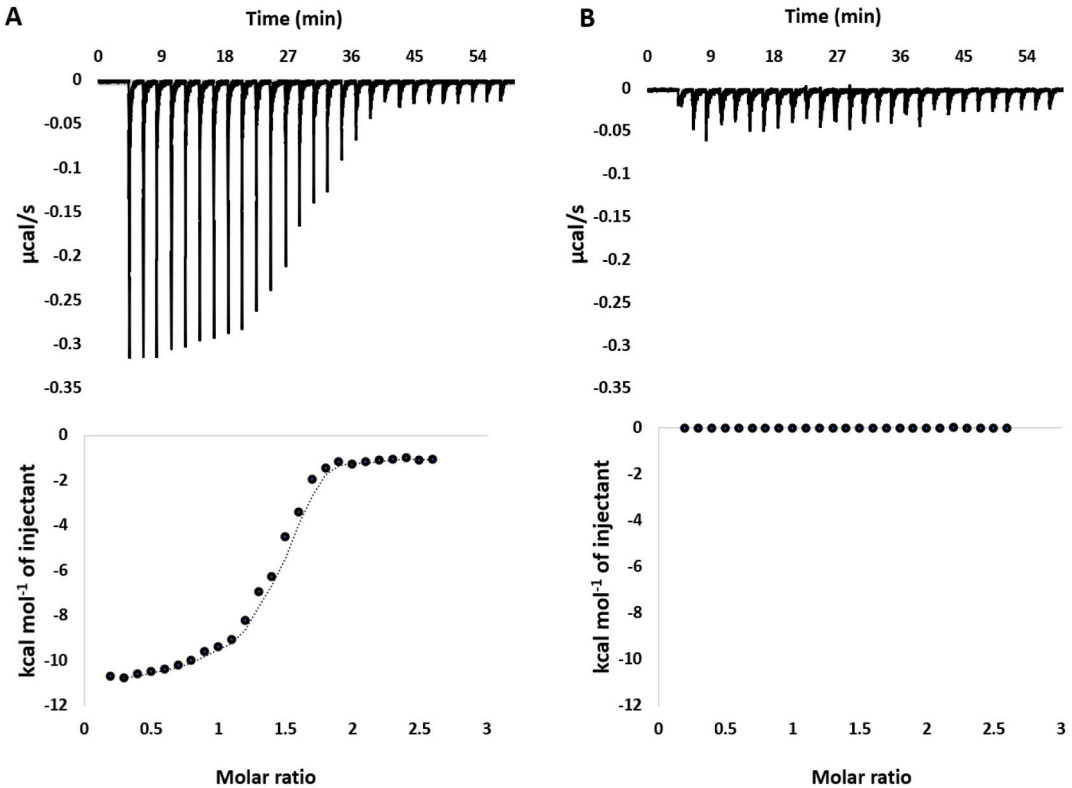

Fig. 3. ITC analysis of the LOS's interaction with ACE2 and RBD. Thermograms (upper row) and binding isotherms (lower row) determined from LOS titrations into ACE2 (A) and RBD (B). LOS in each titration was used in a concentration of 2000 nM, and the protein (either ACE2 or RBD) was 50 nM.

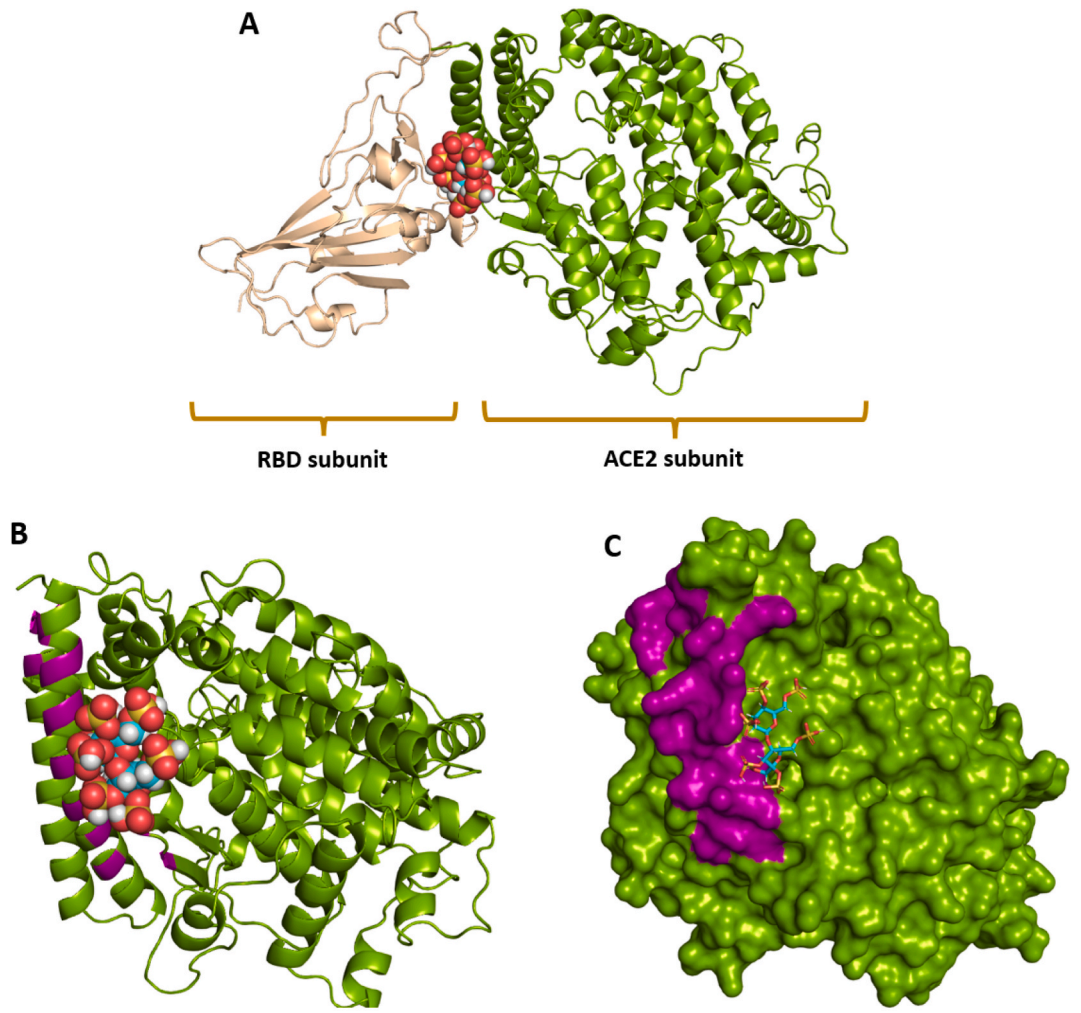

Fig. 4. A: Binding of LOS within the previously characterized binding site (Site A) at the interface of RBD and ACE2. The binding of aloin A [27] inside this binding site has been shown to induce RBD-ACE2 complex dissociation, however binding of LOS did not influence the complex stability. **B** and **C:** Two different representations of ACE2 (green structure) showing the best binding site of LOS (cyan structure). The violet-colored region represents the RBD-binding site. The binding of LOS clearly overlaps with the RBD-binding site.

interface of the RBD-ACE2 complex was able to induce the dissociation of RBD from ACE2 [27].

Similarly, we docked LOS into this binding site (Fig. 4A), and then the resulting poses were subjected to long MD simulations (500 ns) to investigate if the modeled binding of LOS is also capable of destabilizing the RBD-ACE2 complex. The results indicated that such binding (i.e., inside Site A) did not influence the stability of the RBD-ACE2 complex, and hence, this proposed mechanism of interaction failed to explain the LOS-ACE2 binding. Consequently, we directed our investigation to find out the possible binding site of LOS on ACE2 itself.

3.2.2. Mapping LOS's binding sites on ACE2

Since ACE2's protein surface contains numerous putative binding cavities, we set out to find LOS's probable binding sites in a blind fashion, without using any prior knowledge to guide our efforts. Hence, LOS modeled structure was docked into each possible binding site on the ACE2 surface using a docking protocol called "blind docking" [38]. All the resulting binding poses (Fig. S1) were subsequently subjected to quick MD simulations (20 ns-long) to verify the docking poses' stability. By comparing the RMSD values to the corresponding docked postures, we determined the stability of these docking positions during MD simulations. Binding poses with smaller mean RMSD and standard deviation values are more stable. After excluding all bindings that were either not stable and/or located away from the RBD-binding site (Fig. S1), a single binding site was retrieved as a probable binding site for LOS on ACE2. As shown in Fig. 4B and C, the binding of LOS at this proposed binding site overlaps with the RBD-binding site indicating that if LOS can achieve stable binding inside this site, it will make the RBD-binding site inaccessible to RBD, and hence, block one of the major entry points of coronaviruses (i.e., ACE2).

Long MD simulations (300 ns-long; $n = 3$) were then carried out using the proposed binding pose of LOS. As depicted in Fig. 5A and

B, LOS established a stable binding inside this proposed binding site over the course of the simulation with low fluctuations and RMSDs (average RMSD ~ 1.8 Å). The calculated absolute binding free energy ($\Delta G_{Binding}$) was found to be comparable with the experimental one ($\Delta G_{Binding} = -9.49 \pm 0.47$ kcal/mol) indicating very good binding affinity.

The most populated binding pose was then extracted from the MD trajectories to examine the interactions of LOS inside the proposed binding site. As shown in Fig. 5A and B, electrostatic interactions between the LOS's sulfate groups and the cationic amino acid residues (LYS-353, ARG-393, and HIS-34) were the key interactions. In addition, there were other hydrophilic interactions in terms of H-bonding with ASP-30, ASN-33, GLU-37, and ALA-387.

Accordingly, it can be concluded that the binding of LOS with ACE2 is likely via this proposed binding site.

3.2.3. *Gaussian accelerated molecular dynamics (GaMD) simulations*

The binding pathway of LOS to the predicted binding site of ACE2 was investigated using four separate *G*aMD simulations. Five copies of the LOS structure were simulated in the solvent box at a distance of at least 20 Å from the modeled ACE2 structure in each simulation lasting 400 ns. After 115.92 ns in one of the simulations, ligand binding was seen, and the ligand remained bound to ACE2 throughout the simulation (Fig. 6A). The top-scoring docking pose was almost identical to the final binding state (RMSD = 1.63 Å; Fig. 6B), suggesting that this is the most likely binding mode of LOS with ACE2.

4. Discussion

Over the past three years, various antiviral screening initiatives have been established in the hope of finding a cure for COVID-19, and currently, the preparation of preventive therapeutics is very important to face the probable next coronavirus pandemic.

The extensive virtual screening method, covering both synthetic and natural compounds, was enabled by the detailed analysis of SARS CoV-2 proteins. Targeting the main viral proteases, like M^{Pro} and PL^{Pro}, has been a primary focus for developing potential anti-SARS CoV-2 drugs. Paxlovid, a recently authorized oral medication for COVID-19, acts as an inhibitor of the SARS CoV-2 M^{Pro} [39].

To counteract the virus's constant mutation, however, we need new therapeutic that work in other unusual modes of action.

Many viruses, including coronaviruses, utilize sulfated polysaccharides, such as heparan sulfate, as a coreceptor for attaching to cells. The process of viral entry and subsequent infection begins with a sequence of interactions, the initial step being the attachment of a viral protein to these heparan sulfate-like polysaccharides present on the cell surface. In addition to its anticoagulant qualities, it is gaining popularity as a coronavirus therapy [40,41].

Immunogenicity [42,43] and poor pharmacokinetic properties are the main drawbacks of employing sulfated polysaccharides as therapeutic antiviral drugs [44]. For instance, in vivo injection of many antiviral carrageenan derivatives has been linked to the

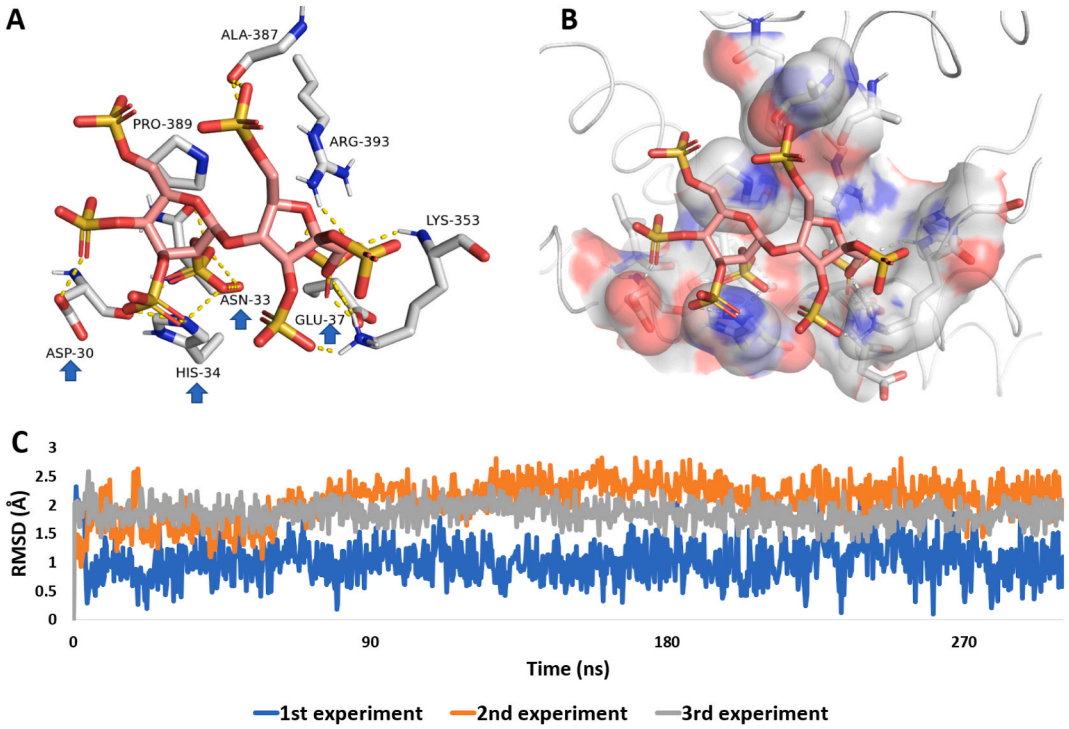

Fig. 5. A and B: show the hypothesized binding mechanism of LOS within ACE2. The blue arrows point to the specific amino acids that interact with the SARS CoV-2 RBD during the binding process. **Figure C** shows the root-mean-square deviation (RMSD) profile of LOS inside the putative binding site for ACE2 throughout the course of 300 ns of MD simulations (3 separate trials).

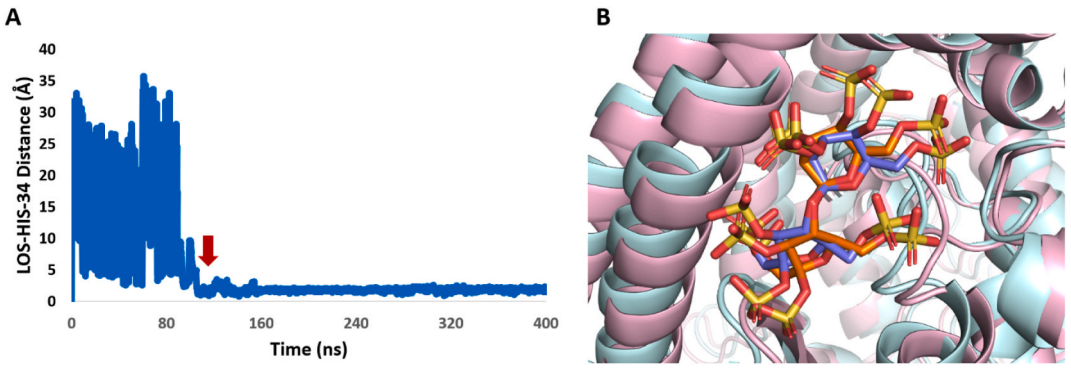

Fig. 6. **A:** After 106 ns in a GaMD simulation, the binding event of LOS with the ACE2 binding site was seen (the red arrow denotes the start of the binding event). **B:** The docking pose of LOS (orange structure) aligned with its most populated structure after binding to the active site of ACE2 (blue structure) using *G*aMD. The root mean square deviation (RMSD) is 1.63 Å. On Zenodo platform, at https://zenodo.org/record/8097049, you can watch a video depicting the binding event of LOS inside the proposed binding site of ACE2.

induction of an acute inflammatory response. It was hypothesized that carrageenan's intrinsic immunogenic structure was linked to this systemic inflammatory response [44,45].

It has been demonstrated that short-chain sulfated polysaccharides including sulfated disaccharides are able to achieve this equilibrium (i.e., high antiviral activity with low toxicity) by decreasing their molecular weight. For instance, studies have demonstrated that chain reduction preserves the antiviral action and minimizes the negative effects of heparin, a naturally occurring sulfated polysaccharide that acts as an anticoagulant [46]. Several follow-up investigations using short-chain sulfated polysaccharides have reached similar conclusions [47,48]. When compared to long chain sulfated polysaccharides, short chain sulfated polysaccharides exhibit improved pharmacokinetic characteristics and reduced immunogenicity.

Herein, we found out that the sulfated disaccharide LOS have broad-spectrum antiviral activity against three coronaviruses (i.e., SARS-CoV-2, SARS-CoV, and MERS-CoV), and its cytotoxicity was significantly low. Taking into consideration the very high polarity of LOS, we postulated that its mode of action might be outside the host cell because such a hydrophilic compound was not able to cross the cellular membrane. Accordingly, the ACE2-S-protein axis was suggested as the main target for LOS. Upon testing the effect of LOS on the affinity of SARS-CoV-2's RBD towards ACE2 by BLI-based experiments, it was found that the binding affinity between the two proteins was significantly reduced in the presence of LOS and this affinity reduction was a dose-dependent.

Furthermore, ITC-based experiments revealed that LOS can bind tightly to ACE2, but not to RBD, showing that LOS can prevent coronavirus entry regardless of strain type, making it an excellent candidate for current and future SARS-CoV emergency scenarios.

As a safety measure, we determined if LOS has an inhibitory activity against ACE2, and we found that LOS did not inhibit the ACE2 catalytic activity up to 100 μM. This finding also indicated that LOS bind with ACE2 via an allosteric binding site far away its active site.

The in silico investigations revealed that the probable binding site of LOS on the ACE2 structure overlaps with the RBD-binding site, explaining all of the previously discussed in vitro observations. Further *G*aMD trials were able to establish a simulated binding event between LOS and ACE2, with the final binding state of LOS being nearly identical to that obtained from docking experiments.

Recent research [49–54] has shown that various agents, including small molecules, proteins, and antibodies, are capable of obstructing the RBD-ACE2 binding. Many of these investigations have yielded similar results, with a majority employing comprehensive molecular dynamics (MD) simulations to examine the stabilizing and destabilizing impacts of these agents.

The primary limitation of the current study is the absence of in vivo evaluation of LOS. Consequently, future research is planned to assess this molecule in vivo, potentially using a nano-formulation (such as an inhaled powder or spray) to enhance its bioavailability and localize its antiviral effects.

5. Conclusion and future scope

This study has successfully demonstrated the antiviral efficacy of Lactulose octasulfate (LOS) against prominent coronaviruses, including SARS-CoV-2. Our findings show that LOS significantly reduces the binding affinity of the SARS-CoV-2 receptor-binding domain (RBD) to ACE2. This suggests a potential mechanism of action through which LOS interferes with the virus-host cell interaction. The findings are supported by comprehensive biolayer interferometry, isothermal titration calorimetry, and Gaussian accelerated molecular dynamics simulations. The ability of LOS to bind ACE2 without inhibiting its enzymatic activity positions it as a promising candidate for the development of effective treatments against SARS-CoV-2 and potentially other coronavirus strains.

The promising results from this study pave the way for several future research directions. Validating the efficacy and safety of LOS in in vivo models is the immediate next step, which will provide insights into its pharmacodynamics, pharmacokinetics, and therapeutic index. Subject to successful in vivo outcomes, clinical trials would be the next phase to assess LOS's effectiveness in human subjects, especially focusing on dosage, administration routes, and potential side effects. It is also crucial to investigate the effectiveness of LOS against a wider range of coronavirus strains, including emerging variants, to establish its potential as a broad-spectrum

antiviral agent. A deeper understanding of LOS's mechanism of action, particularly its interaction with the ACE2 receptor and its potential effects on viral mutation, is necessary for the development of more effective antiviral strategies. Additionally, exploring the use of LOS in combination with other antiviral agents could offer a more comprehensive approach to treating coronavirus infections. Finally, assessing the long-term impact of LOS treatment on patients, particularly those with varying infection severities and comorbidities, is vital for its application in diverse clinical scenarios.

In conclusion, our study opens new avenues for antiviral research against coronaviruses and lays the groundwork for future investigations into LOS and similar compounds. The results of this study advocate for a continued and expanded exploration into LOS's potential as a novel and effective treatment strategy in the ongoing global battle against coronavirus-related diseases.

Data availability

No data associated with this study has been deposited into a publicly available repository. Data included in article/supp. Material/ referenced in the article.

Additional information

No additional information is available for this paper.

CRediT authorship contribution statement

Rami Adel Pashameah: Methodology, Funding acquisition. **Raya Soltane:** Investigation, Funding acquisition, Formal analysis. **Ahmed M. Sayed:** Writing – original draft, Project administration, Methodology, Conceptualization.

Declaration of competing interest

The authors declare that they have no known competing financial interests or personal relationships that could have appeared to influence the work reported in this paper.

Acknowledgment

The authors would like to thank the Deanship of Scientific Research at Umm Al-Qura University for supporting this work by Grant Code: (22UQU4320141DSR03).

Appendix A. Supplementary data

Supplementary data to this article can be found online at https://doi.org/10.1016/j.heliyon.2023.e23222.

References

[1] O.J. Watson, G. Barnsley, J. Toor, A.B. Hogan, P. Winskill, A.C. Ghani, Global impact of the first year of COVID-19 vaccination: a mathematical modelling study, Lancet Infect. Dis. 22 (2022) 1293–1302.
[2] A.A. Alghamdi, Impact of the COVID-19 pandemic on the social and educational aspects of Saudi university students' lives, PLoS One 16 (2021), e0250026.
[3] L. Ameen, H. Assaggaf, R. Alsafi, F. Minshawi, S. Alghamdi, Alharbi, B. Alsaif, Analysis of the clinical characteristics of COVID-19 patient severity amongst Saudi hospital admission in 2020, J. Umm Al-Qura Univ. Med. Sci. 8 (2022) 18–23.
[4] S.A. Amin, S. Banerjee, K. Ghosh, S. Gayen, T. Jha, Protease targeted COVID-19 drug discovery and its challenges: insight into viral main protease (M^{pro}) and papain-like protease (PLpro) inhibitors, Bioorg. Med. Chem. 29 (2021), 115860.
[5] H. Li, Y. Zhou, M. Zhang, H. Wang, Q. Zhao, J. Liu, Updated approaches against SARS-CoV-2, antimicrob, Agents Chemother 64 (2020).
[6] A.S. Alkhamiss, A. Alodheilah, R. Alzaghran, K. Alfurayh, F. Alsultan, R. Alshamlan, W. Al Abdulmonem, Impact of exercise on covid-19 patients in Saudi arabia, Umm Al-qura univ, Med. Sci. 5 (2022) 18–23.
[7] S.A. Kemp, D.A. Collier, R.P. Datir, I.A. Ferreira, S. Gayed, A. Jahun, M. Hosmillo, C. Rees-Spear, P. Mlcochova, I.U. Lumb, SARS-CoV-2 evolution during treatment of chronic infection, Nature 592 (2021) 277–282.
[8] P. Monk, R. Marsden, V. Tear, J. Brookes, T. Batten, M. Mankowski, F. Gabbay, D. Davies, S. Holgate, L. Ho, Inhaled Interferon Beta COVID-19 Study Group Safety and efficacy of inhaled nebulised interferon beta-1a (SNG001) for treatment of SARS-CoV-2 infection: a randomised, double-blind, placebo-controlled, phase 2 trial, Lancet Respir. Med. 9 (2021) 196–206.
[9] R.C. Group, Dexamethasone in hospitalized patients with Covid-19, N. Engl. J. Med. 384 (2021) 693–704.
[10] A.S. Anderson, P. Caubel, J.M. Rusnak, Nirmatrelvir–ritonavir and viral load rebound in COVID-19, N. Engl. J. Med. 387 (2022) 1047–1049.
[11] H. Cheng, Y. Wang, G.Q. Wang, Organ-protective effect of angiotensin-converting enzyme 2 and its effect on the prognosis of COVID-19, J. Med. Virol. 92 (7) (2020) 726–730.
[12] F. Li, W. Li, M. Farzan, S.C. Harrison, Structure of SARS coronavirus spike receptor-binding domain complexed with receptor, Science 309 (5742) (2005) 1864–1868.
[13] H.A. Rothan, S.N. Byrareddy, The epidemiology and pathogenesis of coronavirus disease (COVID-19) outbreak, J. Autoimmun. 109 (2020), 102433.
[14] R. Yan, Y. Zhang, Y. Li, L. Xia, Y. Guo, Q. Zhou, Structural basis for the recognition of SARS-CoV-2 by full-length human ACE2, Science 367 (6485) (2020) 1444–1448.

[15] X. Ou, Y. Liu, X. Lei, P. Li, D. Mi, L. Ren, Z. Qian, Characterization of spike glycoprotein of SARS-CoV-2 on virus entry and its immune cross-reactivity with SARS-CoV, Nat. Commun. 11 (1) (2020) 1620.
[16] K. Sriram, P.A. Insel, Risks of ACE inhibitor and ARB usage in COVID-19: evaluating the evidence, Clinical Pharmacology & Therapeutics 108 (2) (2020) 236–241.
[17] P.S. Kwon, H. Oh, S.J. Kwon, W. Jin, F. Zhang, K. Fraser, J.S. Dordick, Sulfated polysaccharides effectively inhibit SARS-CoV-2 in vitro, Cell discovery 6 (1) (2020) 50.
[18] S. Song, H. Peng, Q. Wang, Z. Liu, X. Dong, C. Wen, B. Zhu, Inhibitory activities of marine sulfated polysaccharides against SARS-CoV-2, Food Funct. 11 (9) (2020) 7415–7420.
[19] M. Andrew, G. Jayaraman, Marine sulfated polysaccharides as potential antiviral drug candidates to treat Corona Virus disease (COVID-19), Carbohydr. Res. 505 (2021), 108326.
[20] S.E. Guimond, C.J. Mycroft-West, N.S. Gandhi, J.A. Tree, T.T. Le, C.M. Spalluto, J.E. Turnbull, Synthetic heparan sulfate mimetic pixatimod (PG545) potently inhibits SARS-CoV-2 by disrupting the spike–ACE2 interaction, ACS Cent. Sci. 8 (5) (2022) 527–545.
[21] S. Song, H. Peng, Q. Wang, Z. Liu, X. Dong, C. Wen, B. Zhu, Inhibitory activities of marine sulfated polysaccharides against SARS-CoV-2, Food Funct. 11 (9) (2020) 7415–7420.
[22] M.A. Skidmore, S.E. Guimond, A.F. Dumax-Vorzet, E.A. Yates, J.E. Turnbull, Disaccharide compositional analysis of heparan sulfate and heparin polysaccharides using UV or high-sensitivity fluorescence (BODIPY) detection, Nat. Protoc. 5 (12) (2010) 1983–1992.
[23] G. Froldi, F. Baronchelli, E. Marin, M. Grison, Antiglycation activity and HT-29 cellular uptake of aloe-emodin, aloin, and aloe arborescens leaf extracts, Molecules 24 (11) (2019) 2128.
[24] A.E. Salih, B. Thissera, M. Yaseen, A.S. Hassane, H.R. El-Seedi, A.M. Sayed, M.E. Rateb, Marine sulfated polysaccharides as promising antiviral agents: a comprehensive report and modeling study focusing on SARS CoV-2, Mar. Drugs 19 (8) (2021) 406.
[25] S. Borkotoky, D. Dey, Z. Hazarika, Interactions of angiotensin-converting enzyme-2 (ACE2) and SARS-CoV-2 spike receptor-binding domain (RBD): a structural perspective, Mol. Biol. Rep. 50 (3) (2023) 2713–2721.
[26] C.K. Oh, T. Nakamura, N. Beutler, X. Zhang, J. Piña-Crespo, M. Talantova, S.A. Lipton, Targeted protein S-nitrosylation of ACE2 inhibits SARS-CoV-2 infection, Nat. Chem. Biol. 19 (3) (2023) 275–283.
[27] H.A. Alhadrami, A.M. Sayed, H.M. Hassan, M.E. Rateb, Aloin A inhibits SARS CoV-2 replication by targeting its binding with ACE2-Evidence from modeling-supported molecular dynamics simulation, J. Biomol. Struct. Dyn. (2023) 1–10.
[28] K. Ochi, Y. Watanabe, K. Okui, M. Shindo, Crystalline salts of sucrose octasulfate, Chem. Pharm. Bull. 28 (2) (1980) 638–641.
[29] T.J.J.I.M. Mosdam, Rapid colorimetric assay for cellular growth and survival: application to proliferation and cytotoxic assay, J. Immunol. Methods 65 (1983) 55–63.
[30] T. Xiao, J. Lu, J. Zhang, R.I. Johnson, L.G. McKay, N. Storm, B. Chen, A trimeric human angiotensin-converting enzyme 2 as an anti-SARS-CoV-2 agent, Nat. Struct. Mol. Biol. 28 (2) (2021) 202–209.
[31] Y. Chen, Y.N. Zhang, R. Yan, G. Wang, Y. Zhang, Z.R. Zhang, C. Wang, ACE2-targeting monoclonal antibody as potent and broad-spectrum coronavirus blocker, Signal Transduct. Targeted Ther. 6 (1) (2021) 315.
[32] A. Kramer, M. Eggers, M. Exner, N.O. Hübner, A. Simon, E. Steinmann, P. Zwicker, Recommendation of the German Society of Hospital Hygiene (DGKH): Prevention of COVID-19 by Virucidal Gargling and Virucidal Nasal Spray–Updated Version April 2022, vol. 17, GMS hygiene and infection control, 2022.
[33] A. Kramer, M. Eggers, N.O. Hübner, P. Walger, E. Steinmann, M. Exner, Virucidal gargling and virucidal nasal spray, GMS Hygiene and Infection Control 16 (2021).
[34] S.E. Guimond, C.J. Mycroft-West, N.S. Gandhi, J.A. Tree, T.T. Le, C.M. Spalluto, J.E. Turnbull, Synthetic heparan sulfate mimetic pixatimod (PG545) potently inhibits SARS-CoV-2 by disrupting the spike–ACE2 interaction, ACS Cent. Sci. 8 (5) (2022) 527–545.
[35] J. Sun, S. Song, C. Ai, B. Zhu, J. Yang, A sulfated abalone polysaccharide inhibited SARS-CoV-2 infection of Vero E6 cells in vitro, Foods 11 (18) (2022) 2865.
[36] K. Ochi, Y. Watanabe, K. Okui, M. Shindo, Crystalline salts of sucrose octasulfate, Chem. Pharm. Bull. 28 (2) (1980) 638–641.
[37] C. Wang, S. Wang, D. Li, D.Q. Wei, J. Zhao, J. Wang, Human intestinal defensin 5 inhibits SARS-CoV-2 invasion by cloaking ACE2, Gastroenterology 159 (3) (2020) 1145–1147.
[38] C. Hetényi, D. van der Spoel, Blind docking of drug-sized compounds to proteins with up to a thousand residues, FEBS Lett. 580 (5) (2006) 1447–1450.
[39] E.N. Muratov, et al., A critical overview of computational approaches employed for COVID-19 drug discovery, Chem. Soc. Rev. 50 (16) (2021) 9121–9151, https://doi.org/10.1039/D0CS01065K.
[40] V. Cagno, E.D. Tseligka, S.T. Jones, C. Tapparel, Heparan sulfate proteoglycans and viral attachment: true receptors or adaptation bias? Viruses 11 (7) (2019) 596.
[41] U. Lindahl, J.P. Li, Heparin–an old drug with multiple potential targets in Covid-19 therapy, J. Thromb. Haemostasis 18 (9) (2020) 2422–2424.
[42] L. Huang, M. Shen, G.A. Morris, J. Xie, Sulfated polysaccharides:Immunomodulation and signaling mechanisms, Trends Food Sci. Technol. 92 (2019) 1–11.
[43] S. Patel, Seaweed-derived sulfated polysaccharides: scopes and challenges in implication in health care, in: Bioactive Seaweeds for Food Applications, Academic Press, 2018, pp. 71–93.
[44] Ø. Arlov, D. Rütsche, M. Asadi Korayem, E. Öztürk, M. Zenobi-Wong, Engineered sulfated polysaccharides for biomedical applications, Adv. Funct. Mater. 31 (19) (2021), 2010732.
[45] J.V. Martino, J. Van Limbergen, L.E. Cahill, The role of carrageenan and carboxymethylcellulose in the development of intestinal inflammation, Frontiers in Pediatrics 5 (2017) 96.
[46] D.A. Gamache, J.T. Povlishock, E.F. Ellis, Carrageenan-induced brain inflammation: characterization of the model, J. Neurosurg. 65 (5) (1986) 679–685.
[47] M. Sundaram, Y. Qi, Z. Shriver, D. Liu, G. Zhao, G. Venkataraman, R. Sasisekharan, Rational design of low-molecular weight heparins with improved in vivo activity, Proc. Natl. Acad. Sci. USA 100 (2) (2003) 651–656.
[48] M. Ciancia, I. Quintana, A.S. Cerezo, Overview of anticoagulant activity of sulfated polysaccharides from seaweeds in relation to their structures, focusing on those of green seaweeds, Curr. Med. Chem. 17 (23) (2010) 2503–2529.
[49] D. Fleita, M. El-Sayed, D. Rifaat, Evaluation of the antioxidant activity of enzymatically-hydrolyzed sulfated polysaccharides extracted from red algae; Pterocladia capillacea, LWT–Food Sci. Technol. 63 (2) (2015) 1236–1244.
[50] M. Razizadeh, M. Nikfar, Y. Liu, Small molecule therapeutics to destabilize the ACE2-RBD complex: a molecular dynamics study, Biophys. J. 120 (14) (2021) 2793–2804.
[51] A. Khan, J. Gui, W. Ahmad, I. Haq, M. Shahid, A.A. Khan, A. Mohammad, The SARS-CoV-2 B. 1.618 variant slightly alters the spike RBD–ACE2 binding affinity and is an antibody escaping variant: a computational structural perspective, RSC advances 11 (48) (2021) 30132–30147.
[52] S. Teng, A. Sobitan, R. Rhoades, D. Liu, Q. Tang, Systemic effects of missense mutations on SARS-CoV-2 spike glycoprotein stability and receptor-binding affinity, Briefings Bioinf. 22 (2) (2021) 1239–1253.
[53] J. Verma, N. Subbarao, Insilico study on the effect of SARS-CoV-2 RBD hotspot mutants' interaction with ACE2 to understand the binding affinity and stability, Virology 561 (2021) 107–116.
[54] L. Yang, J. Li, S. Guo, C. Hou, C. Liao, L. Shi, X. He, SARS-CoV-2 variants, RBD mutations, binding affinity, and antibody escape, Int. J. Mol. Sci. 22 (22) (2021), 12114.